U. S. DEPARTMENT OF COMMERCE NATIONAL BUREAU OF STANDARDS

RESEARCH PAPER RP1161

Part of Journal of Research of the National Bureau of Standards, Volume 21, December 1938

STRENGTH OF A RIVETED STEEL RIGID FRAME HAVING A CURVED INNER FLANGE

By Ambrose H. Stang, Martin Greenspan, and William R. Osgood

ABSTRACT

The distribution of stress in the knee of a riveted steel rigid-frame specimen having a curved inner flange was investigated both experimentally and theoretically. A theory was developed which gives the stresses in the knee to the same order of accuracy as the ordinary beam theory gives the stresses in the straight legs of the frame. Reinforcing the outer corner of the knee and stiffening the web were shown to have little effect on the stress distribution in the frame. The maximum load that could be sustained by the specimen was determined.

CONTENTS

		Page
I.	Introduction	853
II.	Rigid-frame specimen	853
	1. Description of the specimen	853
	2. Tensile properties of the material	854
III.	Testing procedure	855
IV.	Measured stresses	856
V.	Analytical determination of the stresses	863
VI.	Theoretical stresses	868
VII.	Maximum load	870
VIII.	Conclusions	870
IX.	References	871

I. INTRODUCTION

Tests have been made, with the cooperation of the American Institute of Steel Construction, on three steel rigid-frame specimens. The results of tests on a riveted specimen having straight flanges [1][a] have been reported in RP1130. The results of tests on a riveted specimen having a curved inner flange are reported here. This specimen was donated by the American Bridge Co. The results of tests on the third specimen will be reported in a later paper.

II. RIGID-FRAME SPECIMEN

1. DESCRIPTION OF THE SPECIMEN

The rigid-frame specimen is shown in figure 1. It was fabricated from steel plates and angles joined by riveting. The weight as determined by the American Bridge Co. was 2,800 lb. The web of

[a] Numbers in brackets indicate the references at the end of this paper.

the specimen was cut from a single plate. The specimen was symmetrical about a line joining the center of the curved flange and the intersection of the straight flanges.

The outer corner of the specimen was reinforced by a gusset on each side secured to the web by rivets. Additional reinforcement at the outer corner was provided by extra angles and a bent plate. These angles and the plate were secured by bolts turned to a light driving fit in reamed holes, as shown in figure 1, and were removed in some of the tests.

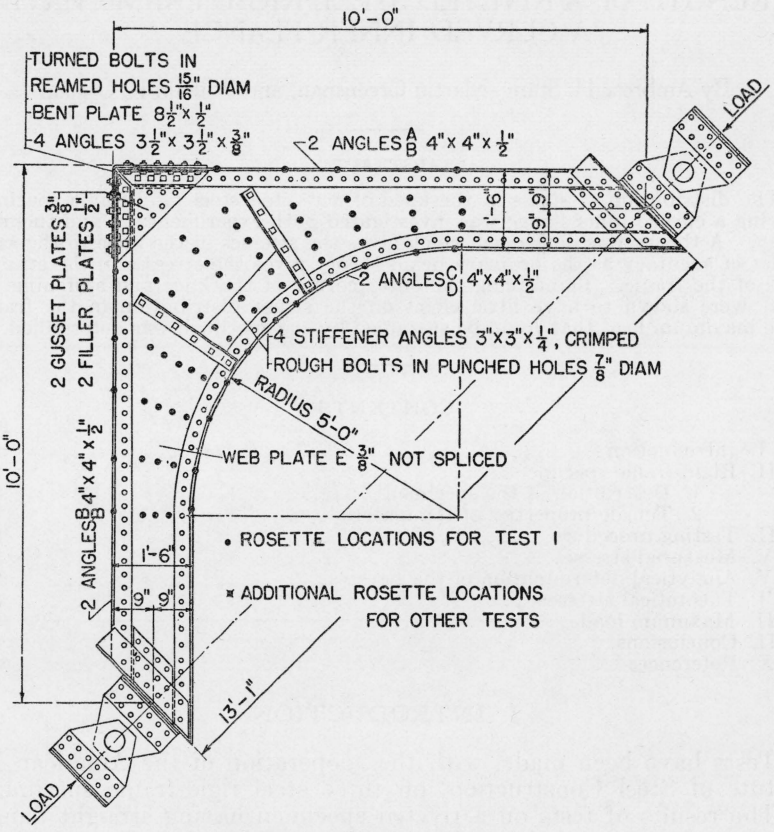

FIGURE 1.—*Rigid-frame specimen.*

The web was stiffened by angles, as shown in figure 1. The lower ends of the stiffener angles were crimped over the connected legs of the inner-flange angles. The stiffener angles were secured to the web and the inner flange of the specimen by rough bolts in punched holes and were removed in one of the tests.

2. TENSILE PROPERTIES OF THE MATERIAL

Samples were taken from the flange angles and web plate before fabrication and marked *A*, *B*, *E*, etc., for identification, as shown in figure 1. The tensile properties of the material were determined from coupons machined from these samples. The coupons were ASTM

8-in.-gage-length tensile specimens for plates, shapes, and flats [2]. The width of the coupons at the reduced section was 1.5 in., and the thickness was that of the material as rolled.

The coupons were tested in a screw-driven, beam-and-poise testing machine having a capacity of 100 kips. The speed of the movable platen of the testing machine was 0.008 in./min until the extensometer was removed from the coupon. Thereafter the speed of the movable platen was 0.4 in./min.

The strains were determined by means of a Ewing extensometer of 8-in. gage length. One division on the scale of this instrument corresponds to a strain of 0.000025. Readings were estimated to 0.1 division.

The yield point was determined by the drop-of-beam method. Young's modulus of elasticity and the proportional limit were determined from difference curves [3].

The tensile properties of the material are given in table 1.

TABLE 1.—*Tensile properties of the material*

Coupon number	Coupon from	Thickness	Young's modulus of elasticity	Proportional limit	Yield point	Tensile strength	Elongation in 8 inches	Reduction of area
		in.	*Kips/in.²*	*Kips/in.²*	*Kips/in.²*	*Kips/in.²*	*Percent*	*Percent*
1	Angle *A*	0.507	28,600	33	36.7	60.3	28.8	57
2	Angle *A*	.502	29,200	36	37.8	61.4	29.8	59
3	Angle *B*	.498	29,400	31	40.2	67.7	27.9	55
4	Angle *B*	.492	27,800	28	40.6	68.2	27.0	62
5	Angle *C*	.497	29,400	31	39.6	65.6	28.3	55
6	Angle *C*	.500	29,600	35	40.8	68.2	28.3	54
7	Angle *D*	.501	29,200	33	40.2	68.5	27.8	55
8	Angle *D*	.495	29,000	33	39.6	67.1	28.8	53
9	Plate *E*	.383	29,600	35	41.0	61.9	29.8	58
10	Plate *E*	.385	28,900	35	40.2	61.7	28.0	53
11	Plate *E*	.390	29,200	35	39.8	61.2	29.9	55
12	Plate *E*	.391	29,000	38	39 7	60.9	29.2	57
Average			29,100					

III. TESTING PROCEDURE

The rigid-frame specimen was loaded in a vertical, screw-driven, beam-and-poise testing machine having a capacity of 600 kips. The load was applied through two pin-connected shoes, shown in figure 1, one attached to each leg of the frame.

Three different tests were made with the load acting along the line indicated in figure 1. For test 1 the bent plate and extra angles at the outer corner and the stiffener angles were bolted to the specimen. For test 2 the bent plate and extra angles at the outer corner were removed, and for test 3 the stiffener angles were also removed. The bolts through the angles were replaced in each case. The gussets at the outer corner were not removed for any of these tests.

Strain-gage readings were taken at rosettes located as shown in figure 1 with Whittemore strain gages having gage lengths of 2 inches. One division on the dial of the strain gage corresponds to a strain of 0.00005. Readings were estimated to 0.1 division. Each rosette consisted of four gage lines intersecting at a point and inclined at 45° to one another.

Each rosette location on the web shown in figure 1 represents two rosettes, one on either side of the specimen; and each rosette location on the angles represents four rosettes, one on the inside and one on the outside of the outstanding leg of each angle.

The specimen is shown in the testing machine for test 1 in figure 2. Before any strain-gage readings were taken, a compressive load of 67 kips was applied and released five times. Strain-gage readings were taken at compressive loads of 5 kips and 65 kips.

IV. MEASURED STRESSES

Stresses computed from the strain-gage readings will be called measured stresses. These stresses were computed from the strains[b] due to the 60-kip increase in load by the methods outlined in RP1130 [1]. The strains in corresponding gage lines of rosettes on opposite sides of the web of the specimen were averaged and the average values used in the computations. In the case of the outstanding legs of the flange angles, the strains in corresponding gage lines of the four rosettes were averaged and the average values used in the computations. The magnitudes and directions of the principal stresses and of the maximum shearing stress for each set of two or four rosettes were computed.

The results of these computations are shown for test 1 in figures 3 to 6, inclusive. Figure 3 is a contour chart of maximum principal stress. Each contour line is a locus of points of equal maximum principal stress in the plane of stress. The contour lines show only the magnitudes of the stress. The directions of the contour lines are not the directions of the maximum principal stresses. The contour lines do not give the values of the stresses in the stiffeners. Similar contour charts of minimum principal stress and of maximum shearing stress are shown in figures 4 and 5, respectively, except that the contour lines of maximum shearing stress in figure 5 were drawn for the three-dimensional state of stress. At any point at which the principal stresses in the plane of stress are of the same sign, the maximum shearing stress occurs in planes at 45° to the plane of stress and is equal to one-half the numerically larger of these principal stresses. The magnitudes and directions of the principal stresses in the plane of stress are shown in figure 6.

The results of tests 2 and 3 are shown in the same way in figures 7 to 14, inclusive.

[b] The greatest deviation of any value of the modulus of elasticity from the average value was about 4.5 percent (table 1). The average value was used for computing the stresses, because it was estimated that the error in the strain-gage readings was greater than 4.5 percent.

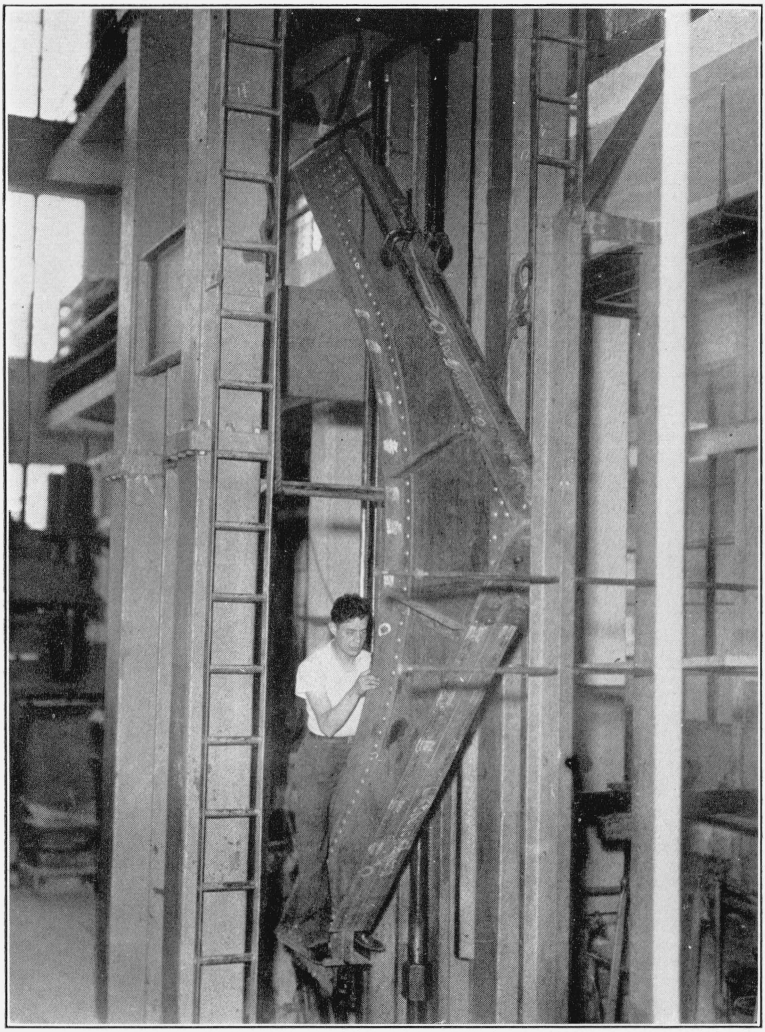

FIGURE 2.—*The rigid-frame specimen in the testing machine.*

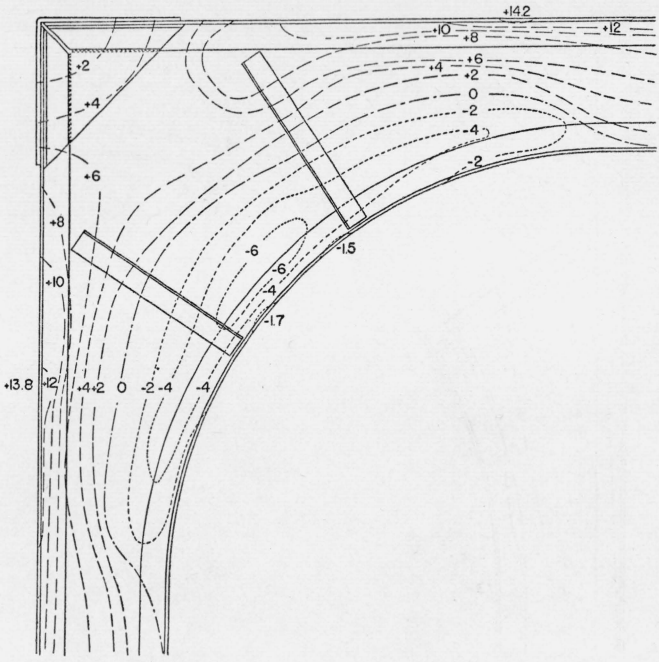

FIGURE 3.—*Test 1.—Maximum principal stress, kips/in*^{2}.

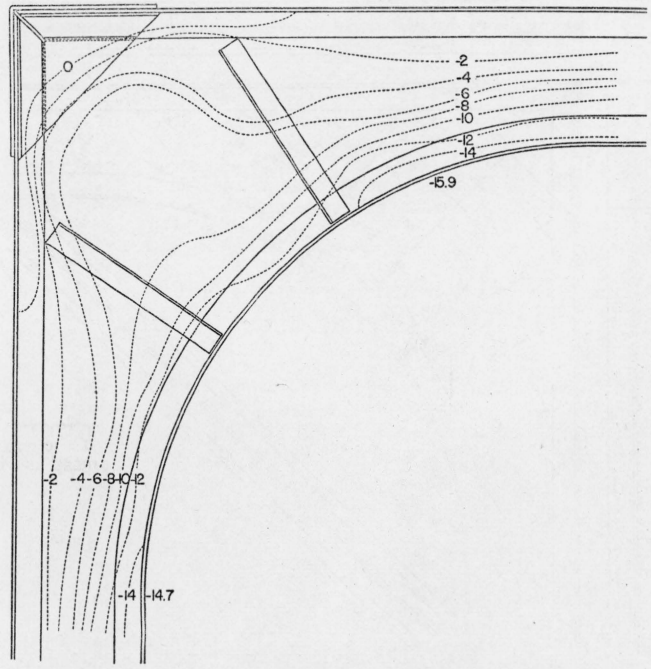

FIGURE 4.—*Test 1.—Minimum principal stress, kips/in*^{2}.

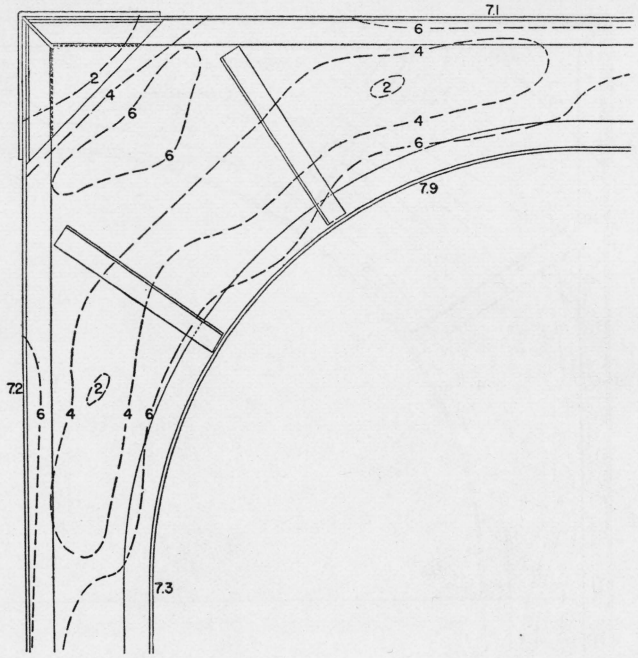

FIGURE 5.—*Test 1.—Maximum shearing stress, kips/in* ^{2}.

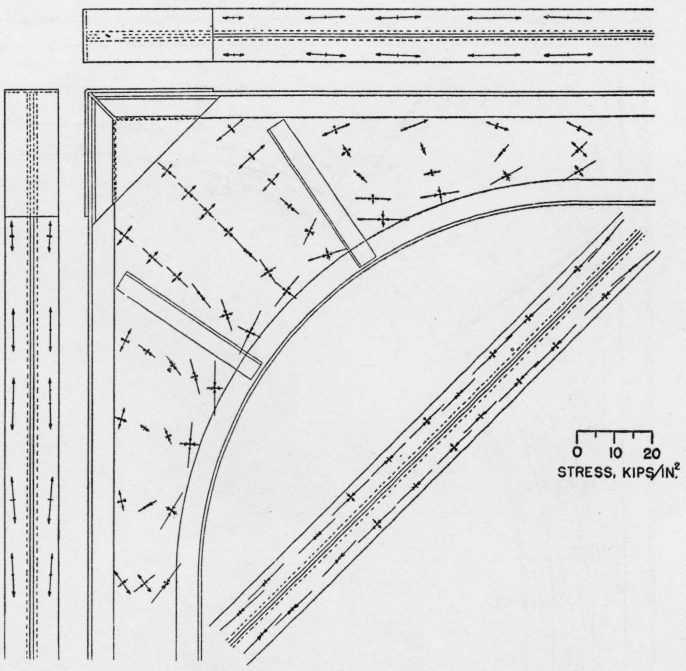

FIGURE 6.—*Test 1.—Magnitude and direction of the maximum and of the minimum principal stresses, kips/in* ^{2}.

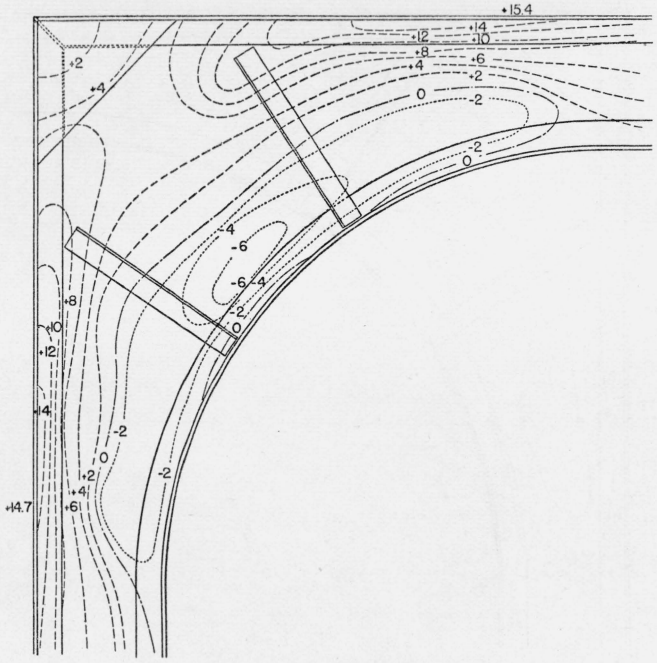

FIGURE 7.—*Test 2.—Maximum principal stress, kips/in* ^{2}.

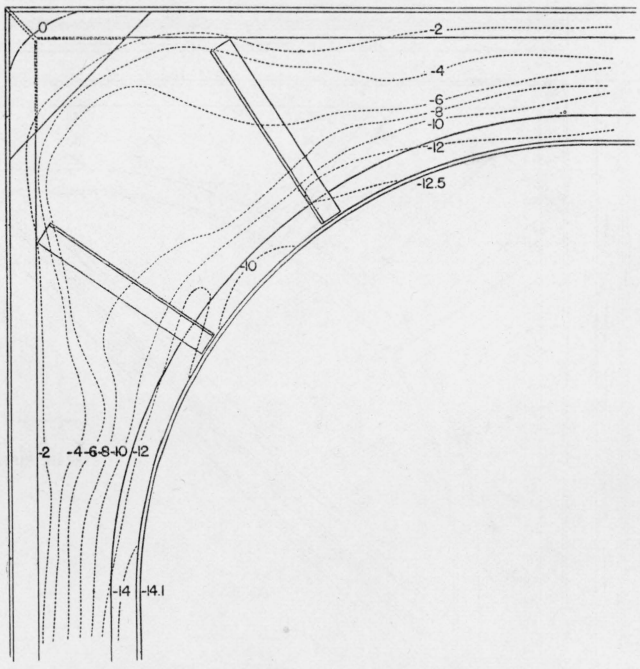

FIGURE 8.—*Test 2.—Minimum principal stress, kips/in* ^{2}.

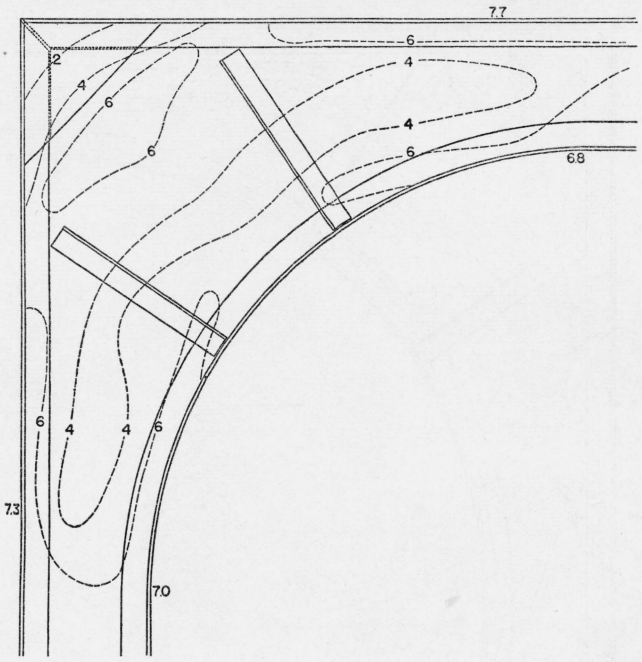

FIGURE 9.—*Test 2.—Maximum shearing stress, kips/in* ^{2}.

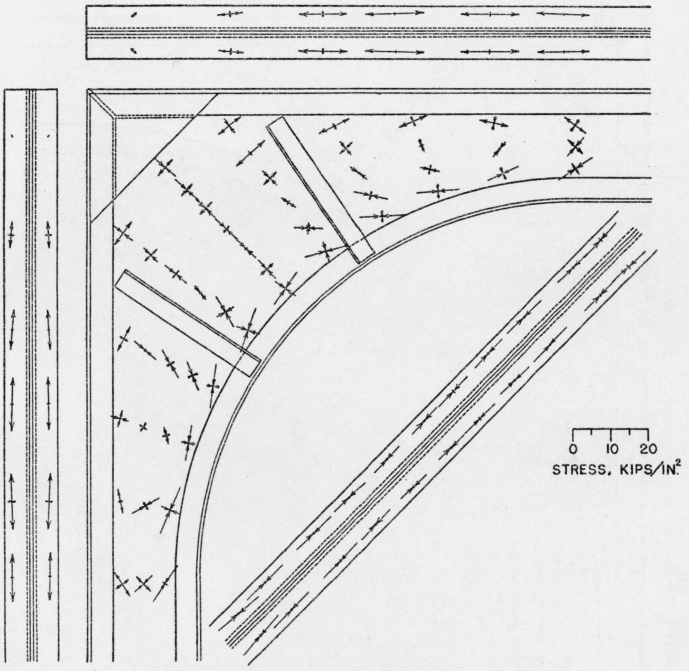

FIGURE 10.—*Test 2.—Magnitude and direction of the maximum and of the minimum principal stresses, kips/in* ^{2}.

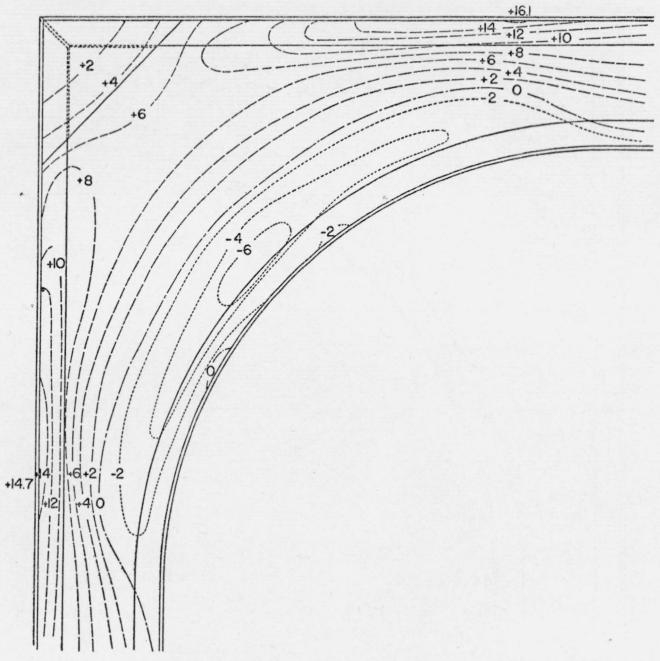

FIGURE 11.—*Test 3.—Maximum principal stress, kips/in* ^{2}.

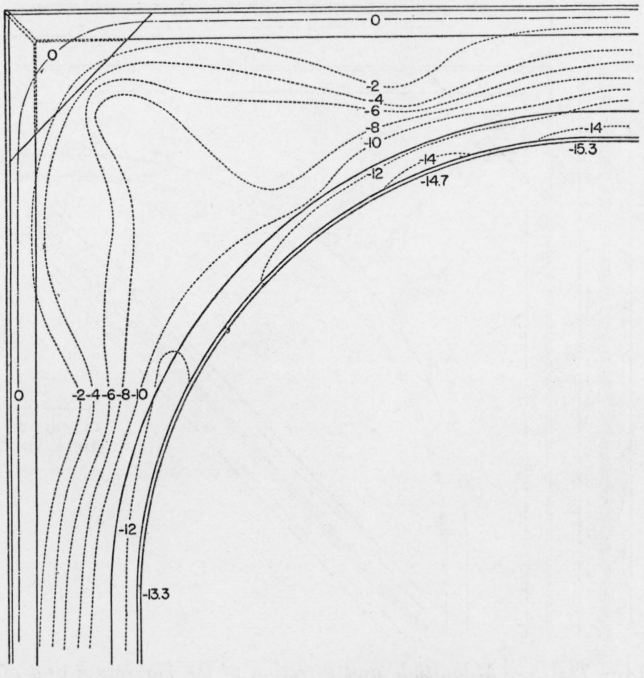

FIGURE 12.—*Test 3.—Minimum principal stress, kips/in* ^{2}.

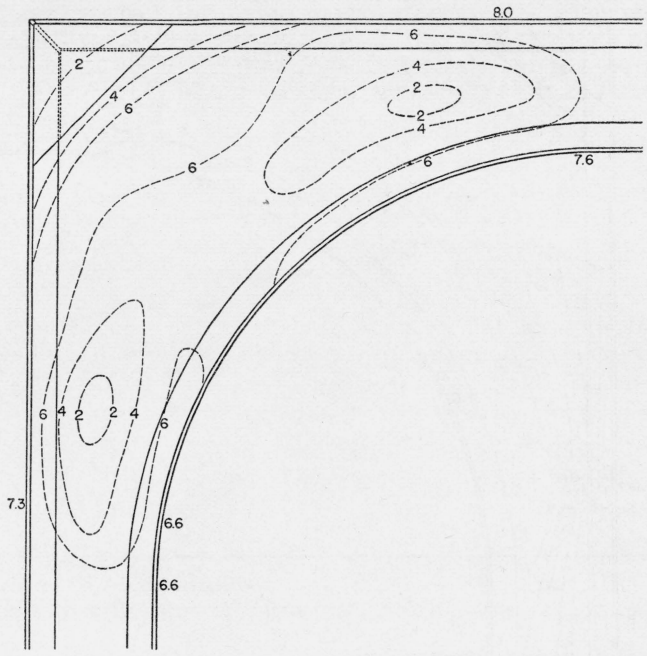

FIGURE 13.—*Test 3.—Maximum shearing stress, kips/in².*

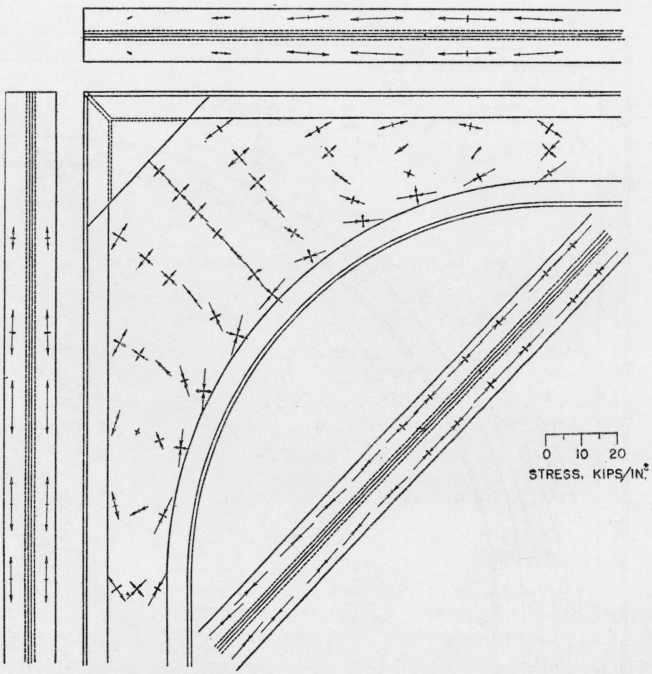

FIGURE 14.—*Test 3.—Magnitude and direction of the maximum and of the minimum principal stresses, kips/in².*

Comparison of the results for the three tests shows that the bent plate and extra angles at the outer corner and the stiffener angles on the web had little effect on the stress distribution in the frame. The stresses at the outer corner were very small.

V. ANALYTICAL DETERMINATION OF THE STRESSES

A rigorous theoretical determination of the state of stress in the knee of a rigid frame with nonparallel curved flanges has not been obtained, but it is possible to determine the stresses semirationally with an accuracy believed to be comparable to that obtained for straight girders by the ordinary formulas used for such girders. Let figure 15 represent the web and the centroidal axes of the flanges of a portion of a rigid frame similar to the specimen tested. Suppose

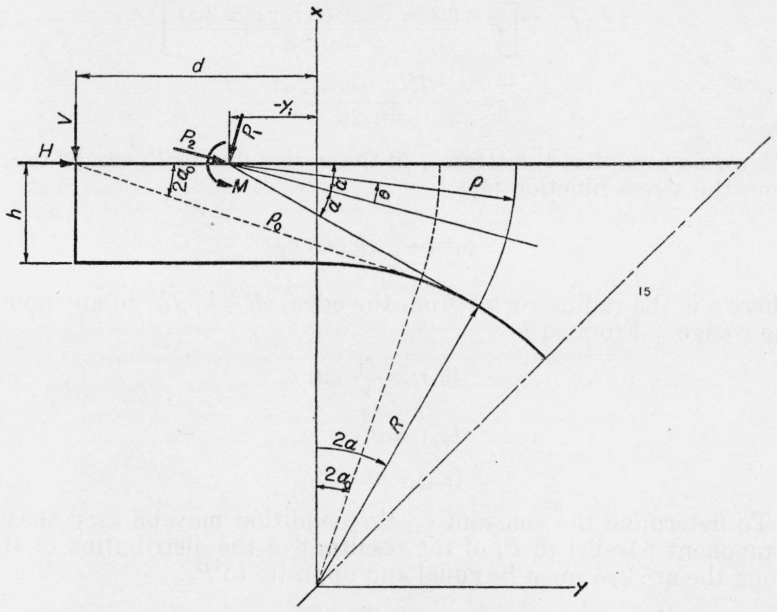

FIGURE 15.—*Web and centroidal axes of flanges of a portion of a rigid frame.*

Determination of circular section and resolution of load at edge of wedge.

the applied load resolved into horizontal and vertical components H and V acting at the centroid of the outer flange at a distance d from the point of tangency of the curved inner flange. Then, with the systems of coordinates shown in the figure, by drawing from any point $(R, 2\alpha)$ of the curved inner flange a tangent intersecting the outer flange at the point $(R+h, y_i)$ it is possible to write semirational expressions for the stresses along the arc, $2\rho\alpha$, swung with center at the intersection, and radius, ρ, equal to the distance between the points $(R+h, y_i)$ and $(R, 2\alpha)$. The radii $\theta=\alpha$, $\theta=-\alpha$, and the arc $2\rho\alpha$ form the boundaries of a wedge, which suggests analysis by means of Airy stress functions. A combination of stress functions is described below by means of which the distribution of stress at the

circular boundary of the wedge may be approximated closely, even though the boundary conditions along the straight boundaries are not all satisfied. The solution for the stresses along the arc $2\rho\alpha$ is very similar to the ordinary one for a girder with parallel flanges and reduces to the latter solution as $\alpha \doteq 0$ ($\rho = \infty$). Its adequacy can be determined only by tests.

In order to obtain the solution, it is convenient to replace the applied load by a force P_1 acting at the point $(R+h, y_i)$ perpendicular to the polar axis $\theta=0$, a force P_2 acting at the same point along the polar axis, and a couple M. These forces and the couple and the radius ρ, which will be required, are easily found to be (see fig. 15)

$$P_1 = V\cos\alpha - H\sin\alpha, \tag{1}$$

$$P_2 = V\sin\alpha + H\cos\alpha, \tag{2}$$

$$M = V\left[d - \frac{h\cos 2\alpha - R(1-\cos 2\alpha)}{\sin 2\alpha}\right], \tag{3}$$

$$\rho = \frac{h+R(1-\cos 2\alpha)}{\sin 2\alpha}. \tag{4}$$

Now assume that the stresses in the wedge due to P_1 can be derived from the stress function [4]

$$\phi_1 = -\frac{c_1}{2} r\theta\cos\theta, \tag{5}$$

where r is the radius vector from the edge, $(R+h, y_i)$, to any point in the wedge. From eq 5

$$(\sigma_r)_1 = \frac{c_1}{r}\sin\theta, \tag{6}$$

$$(\sigma_\theta)_1 = 0, \tag{7}$$

$$(\tau_{r\theta})_1 = 0. \tag{8}$$

To determine the constant c_1, the condition may be used that the component parallel to P_1 of the resultant of the distribution of stress along the arc $2\rho\alpha$ must be equal and opposite to P_1:

$$2A_f\frac{c_1}{\rho}\sin^2\alpha + tc_1\int_{-\alpha}^{\alpha}\sin^2\theta\, d\theta - P_1 = 0, \tag{9}$$

where the cross-sectional area A_f of each flange is assumed concentrated at $\theta=\alpha$ and $\theta=-\alpha$, respectively, and the thickness of the web plate is denoted by t. From eq 9

$$c_1 = \frac{P_1\rho}{t\rho(\alpha-\sin\alpha\cos\alpha)+2A_f\sin^2\alpha},$$

and the stress $(\sigma_\rho)_1$[c] becomes

$$(\sigma_\rho)_1 = \frac{P_1\sin\theta}{t\rho(\alpha-\sin\alpha\cos\alpha)+2A_f\sin^2\alpha}. \tag{10}$$

[c] Owing to the wide discrepancy between the actual and assumed boundary conditions along the sides of the wedge, none of the computed stresses at $r \neq \rho$ have any significance.

Assume next that the stresses in the wedge due to P_2 can be derived from the stress function [4]

$$\phi_2=\frac{a_1}{2}r\theta \sin \theta, \tag{11}$$

from which

$$(\sigma_r)_2=\frac{a_1}{r}\cos \theta, \tag{12}$$

$$(\sigma_\theta)_2=0, \tag{13}$$

$$(\tau_{r\theta})_2=0. \tag{14}$$

To determine the constant a_1 the condition may be used that the resultant of the distribution of stress along the arc $2\ \rho\alpha$ must hold P_2 in equilibrium:

$$2A_f\frac{a_1}{\rho}\cos^2 \alpha+ta_1\int_{-\alpha}^{\alpha} \cos^2 \theta d\theta+P_2=0. \tag{15}$$

From eq 15

$$a_1=-\frac{P_2\rho}{t\rho(\alpha+\sin\ \alpha \cos\ \alpha)+2A_f \cos^2 \alpha},$$

and the stress $(\sigma_\rho)_2$[d] becomes

$$(\sigma_\rho)_2=-\frac{P_2 \cos \theta}{t\rho(\alpha+\sin\ \alpha \cos\ \alpha)+2A_f \cos^2 \alpha}. \tag{16}$$

Assume, finally, that the stress in the wedge due to M can be derived from the stress function

$$\phi_3=a_0'\theta+d_2' \sin 2\theta, \tag{17}$$

from which

$$(\sigma_r)_3=-\frac{4}{r^2}d_2' \sin 2\theta, \tag{18}$$

$$(\sigma_\theta)_3=0, \tag{19}$$

$$(\tau_{r\theta})_3=\frac{1}{r^2}(a_0'+2d_2' \cos 2\theta). \tag{20}$$

Again, by considering the boundary $2\rho\alpha$ of the wedge, the constants may be determined from the condition of equilibrium of forces perpendicular to the polar axis and the condition of equilibrium of moments (with respect to the edge of the wedge):

$$-2A_f\frac{4}{\rho^2}d_2' \sin 2\alpha \sin \alpha-\frac{4t}{\rho}d_2'\int_{-\alpha}^{\alpha} \sin 2\theta \sin \theta\ d\theta$$

$$+\frac{t}{\rho}\int_{-\alpha}^{\alpha}(a_0'+2d_2' \cos 2\theta) \cos \theta\ d\theta=0, \tag{21}$$

$$t\int_{-\alpha}^{\alpha}(a_0'+2d_2' \cos 2\theta)d\theta+M=0. \tag{22}$$

[d] See footnote c.

The solution of the two simultaneous eqs, 21 and 22, for a_0' and d_2' gives

$$a_0'=\frac{M}{t}\frac{\cos 2\alpha-\frac{2A_f}{t\rho}\sin 2\alpha}{\sin 2\alpha-2\alpha\cos 2\alpha+\frac{2A_f}{t\rho}\cdot 2\alpha\sin 2\alpha},$$

$$d_2'=-\frac{M}{2t}\frac{1}{\sin 2\alpha-2\alpha\cos 2\alpha+\frac{2A_f}{t\rho}\cdot 2\alpha\sin 2\alpha},$$

and the stresses $(\sigma_\rho)_3$[e] and $(\tau_{\rho\theta})_3$[f] become

$$(\sigma_\rho)_3=\frac{2M}{t\rho^2}\frac{\sin 2\theta}{\sin 2\alpha-2\alpha\cos 2\alpha+\frac{2A_f}{t\rho}\cdot 2\alpha\sin 2\alpha}, \tag{23}$$

$$(\tau_{\rho\theta})_3=\frac{M}{t\rho^2}\frac{\cos 2\alpha-\frac{2A_f}{t\rho}\sin 2\alpha-\cos 2\theta}{\sin 2\alpha-2\alpha\cos 2\alpha+\frac{2A_f}{t\rho}\cdot 2\alpha\sin 2\alpha}. \tag{24}$$

The final stresses are

$$\sigma_\rho=(\sigma_\rho)_1+(\sigma_\rho)_2+(\sigma_\rho)_3, \tag{25}$$
$$\sigma_\theta=0, \tag{26}$$
$$\tau_{\rho\theta}=(\tau_{\rho\theta})_3. \tag{27}$$

The preceding development makes it possible to determine the state of stress. Of primary practical importance is the determination of the maximum normal and shearing stresses. For any circular section $2\rho\alpha$ the numerically largest normal stress occurs at $\theta=\alpha$ or $\theta=-\alpha$, but the determination of α to make the normal stress a maximum or a minimum is another matter. It is evident that differentiating equation 25 with respect to α, setting the derivative equal to zero, and solving the resulting equation for α involves more than mortal man is likely to accomplish. One must be content with cruder methods. A cantilever girder of uniform strength, with negligible web (latticed construction), loaded only by a transverse force at its end, is triangular in elevation according to the ordinary beam theory. Suppose now that we draw from the point of application of the load in figure 15 a tangent to the curved inner flange, as indicated by the angle $2\alpha_0$. If we neglect the web, it is clear that, by analogy with the girder of uniform strength, the circular section $2\rho_0\alpha_0$ is weaker than any section on either side of it when the effect of only the transverse component, $V\cos\alpha_0-H\sin\alpha_0$, of the applied load is considered. The effect of both the web and the longitudinal component, $V\sin\alpha_0+H\cos\alpha_0$, of the applied load is to shift the weakest section to the left. This shift is likely to be small for most practical cases, but in a questionable case it may be desirable to compute the extreme fiber stresses for $\alpha=0$ (by the ordinary beam theory) and for $\alpha=\alpha_0$ ($M=0$).

[e] See footnote c.
[f] See footnote c.

The stresses for these two values of α are particularly easy to compute and will indicate how rapidly the extreme fiber stress is varying. If the stress for $\alpha=\alpha_0$ is close to the maximum allowable stress, it may be worthwhile to compute the extreme fiber stresses for a value of α intermediate between $\alpha=0$ and $\alpha=\alpha_0$.

The value of α_0 may be obtained by equating the right-hand side of eq 3 to zero and solving for cos 2α:

$$\cos 2\alpha_0=\frac{(h+R)R}{(h+R)^2+d^2}\left\{1+\sqrt{1-\frac{(R^2-d^2)[(h+R)^2+d^2]}{R^2(h+R)^2}}\right\}. \tag{28}$$

The corresponding value of ρ_0 is obtained by substituting the value of α_0 from eq 28 for α in eq 4.

The analytical determination of the maximum shearing stress involves the same sort of difficulties as arise in connection with the maximum normal stress. It is simply out of the question as a practical matter to differentiate eq 27 with respect to α, set the derivative equal to zero, and solve the resulting equation for α. It is almost evident, however, that the shearing stress becomes a maximum on the section defined by $\alpha=0$, and consequently the equation for maximum shearing stress, τ_{max}, on the cross section of a straight girder applies,

$$\tau_{max}=\frac{3(th+4A_f)V}{2(th+6A_f)th}. \tag{29}$$

The expressions 10, 16, 23, and 24 should give good approximations to the stresses in any beam or girder with equal nonparallel flanges so long as the radii of curvature of the flanges are not too small relative to the depth at the section at which the stresses are desired. The expressions 10, 16, 23, and 24 are closely analogous to those which apply for a straight girder with parallel flanges and reduce to the latter as $\alpha\doteq 0$ ($\rho=\infty$). If numerator and denominator of eq 10 are multiplied by ρ^2, then the quantity $P_1\rho$ may be thought of as the bending moment at the circular section, the quantity $\rho \sin\theta$ is the distance of any fiber from the neutral surface (the polar axis), and the denominator is the moment of inertia of the circular sectional area with respect to the neutral surface. It is obvious then that as $\alpha\doteq 0$ ($\rho=\infty$), eq 10 reduces to the ordinary flexure formula. Similarly, if in eq 16 $\theta\doteq 0$ and $\alpha\doteq 0$ ($\rho=\infty$), the equation reduces to

$$(\sigma_\rho)_2=-\frac{P_2}{th+2A_f},$$

which is the familiar expression for the normal stress due to an axially applied load. Equation 23 may be written for small values of θ and α as

$$(\sigma_\rho)_3=\frac{M\theta}{\frac{2}{3}t\rho^2\alpha^3+2A_f\rho\alpha^2},$$

which, with $\rho\alpha=h/2$ and $\rho\theta=z$, reduces to

$$(\sigma_\rho)_3=\frac{Mz}{\frac{1}{12}th^3+2A_f\left(\frac{h}{2}\right)^2}.$$

This equation is again the ordinary flexure formula. For small values of θ and α eq 24 may be written

$$(\tau_{\rho\theta})_3=-\frac{M}{t\rho^2}\frac{\frac{1}{2}\alpha^2-\frac{1}{2}\theta^2+\frac{A_f}{t\rho}\alpha}{\frac{2}{3}\alpha^3+2\frac{A_f}{t\rho}\alpha^2},$$

which, with $\rho\alpha=h/2$ and $\rho\theta=z$, reduces to

$$(\tau_{\rho\theta})_3=-\frac{\left[\frac{t}{2}\left(\frac{h^2}{4}-z^2\right)+A_f\frac{h}{2}\right]\frac{M}{\rho}}{\left[\frac{1}{12}th^3+2A_f\left(\frac{h}{2}\right)^2\right]t}.$$

This equation is the familiar one giving the transverse or longitudinal shearing stress at any point at the distance z from the neutral axis of a straight girder when the shearing force on the cross section in question is M/ρ. In the present case M and ρ are given by eq 3 and 4, and by forming the ratio M/ρ and allowing α to approach zero, it is easily found that $M/\rho=-V$.

VI. THEORETICAL STRESSES

The theory was applied to the portion of the rigid-frame specimen bounded by nonparallel flanges. This portion may be termed the "knee" of the frame, and half of it is shown in figure 15, included between the positive axes of x and y. A flange was regarded as consisting of two angles and a part of the web plate between them, and the area of the flange was considered concentrated at its centroid, which was taken as the boundary of the web. The location of this boundary was computed for the two 4- by 4- by ½-in. angles and the part of the included ⅜-in. plate which extended from the centroid of the flange to the backs of the flange angles, by the method outlined in RP1130 [1]. The distance between the boundary and the backs of the angles was found to be 1.15 in., and the dimensions (figs. 1 and 15) of the portion of the frame to which the theory was applied were taken as $h=18-2(1.15)=15.7$ in. and $R=60+1.15=61.15$ in.

The load line intersected the centroidal axis of the outer flange at an angle of 45° at the point $(R+h, -d)$, where (fig. 1) $d=120-18-60+h/2=49.85$ in. The load was resolved at this point into components $H=V=60\sqrt{2/2}=42.43$ kips.

With these values of h, R, d, H, and V, eq 1, 2, 3, and 4 for P_1, P_2, M, and ρ were solved for four values of α, and the results were substituted in =25, 26, and 27 for the stresses. The sections taken correspond to the following values of 2α: $2\alpha=0$, for which the theory reduces to the ordinary beam theory; $2\alpha=2\alpha_0=15°\ 9'$ obtained by solution of eq 28 and for which $M=0$; $2\alpha=30°$; $2\alpha=45°$.

A comparison between the theoretical and the measured stresses for test 3 is shown in figure 16. The curves represent theoretical stresses, and the arrows, measured stresses. The measured normal and shearing stresses shown were obtained from the following quantities measured at the rosettes: the maximum principal stresses, σ_u; the minimum principal stresses, σ_v; and the angles, ψ, between σ_u,

and the load line. The values of σ_u at corresponding rosettes on either side of the line of symmetry of the frame were averaged, and from, the averages were interpolated the values of σ_u at the points at which the measured stresses are plotted in figure 16. The values of σ_v and ψ at these points were obtained similarly, and from the values of σ_u, σ_v, and ψ at each point the components of stress in the r- and θ-directions were computed. The normal stresses, σ_ρ, are shown on four circular sections on the lower half of figure 16, and in addition, the normal stresses in the flanges have been plotted at right angles to the directions in which they act, with the centroidal axes of the flanges as base lines, to show more clearly the variation of stress along the

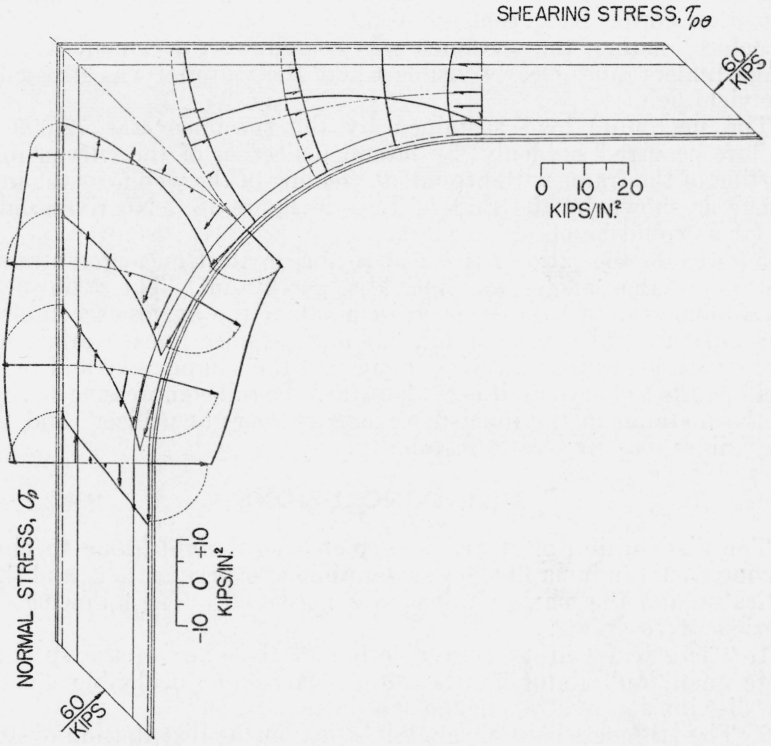

FIGURE 16.—*Test 3.—Theoretical stresses and measured stresses.*
The curves represent theoretical, and the arrows measured, stresses.

flanges. The shearing stresses $\tau_{\rho\theta}$ are plotted on four corresponding sections on the upper half of the figure, and the variation in shearing stress along the center line of the circular sections is also shown.

The agreement between the theoretical stresses and the measured stresses is good, especially for the normal stresses. Except for a few points on the section defined by $2\alpha=45°$, the theory gives stresses to the same order of accuracy as the ordinary beam theory gives the stresses for $2\alpha=0$.

The numerically largest of the measured normal stresses shown in figure 16 occurs at the inner flange on the circular section defined by $\alpha=\alpha_0$. This result is in agreement with the conclusion, drawn

from the theory in section V, that the numerically largest normal stress occurs near the section defined by $\alpha=\alpha_0$. The measured shearing stresses on this section are negligibly small as would be expected from eq 24 and 27, which state that the shearing stresses on this section are everywhere zero.

VII. MAXIMUM LOAD

The rigid-frame specimen is shown in figure 17 in the testing machine for determining the maximum load. The conditions for this test were the same as for test 3, except that lateral deflection of the outer corner of the specimen was prevented, and that the gussets at the outer corner had been removed.[9]

Before loading, the specimen was coated with a cement wash to make Lüders' lines clearly visible where the material was stressed to the yield point.

The maximum load sustained by the specimen was 72,000 lb. Failure occurred suddenly, by lateral deflection of the curved inner portion of the frame with attendant yielding of the web near the inner flange as shown by the Lüders' lines in figure 18. No rivets failed so far as could be observed visually.

For test 3, the ratio of the load to the greatest measured stress in the inner-flange angles was 3.92 kips per kip/in^2. The ratio of the maximum load to the tensile yield point of the angles (see table 1) was only 1.80 kips per kip/in^2. If one assumes linear variation of stress with load up to the yield point and the compressive and tensile yield points to be equal, it is evident that the full compressive strength of the material in the inner-flange angles was not utilized, and that the failure was by elastic instability.

VIII. CONCLUSIONS

The distribution of stress in a riveted steel rigid-frame specimen having a curved inner flange was determined experimentally and theoretically, and the maximum load was measured. The following conclusions were drawn:

1. The stresses at the outer corner of the knee of the specimen were small, and reinforcing the outer corner had a negligible effect on the distribution of stress in the specimen.
2. The stiffeners had a negligible effect on the distribution of stress in portions of the frame not near the stiffeners.
3. The formulas developed give the stresses in the knee to the same order of accuracy as the ordinary beam theory gives the stresses in the straight legs of the frame. These formulas reduce to the ordinary beam theory at the section where the straight and curved parts of the inner flange are tangent.
4. The design was such that the frame failed by elastic instability. The inner-flange angles at failure were stressed to less than half their yield point. This emphasizes the necessity of providing adequate bracing for the inner flange at the knees of rigid frames of this type.

[9] The gussets had been removed in preparation for a contemplated test to determine the stress distribution for this condition.

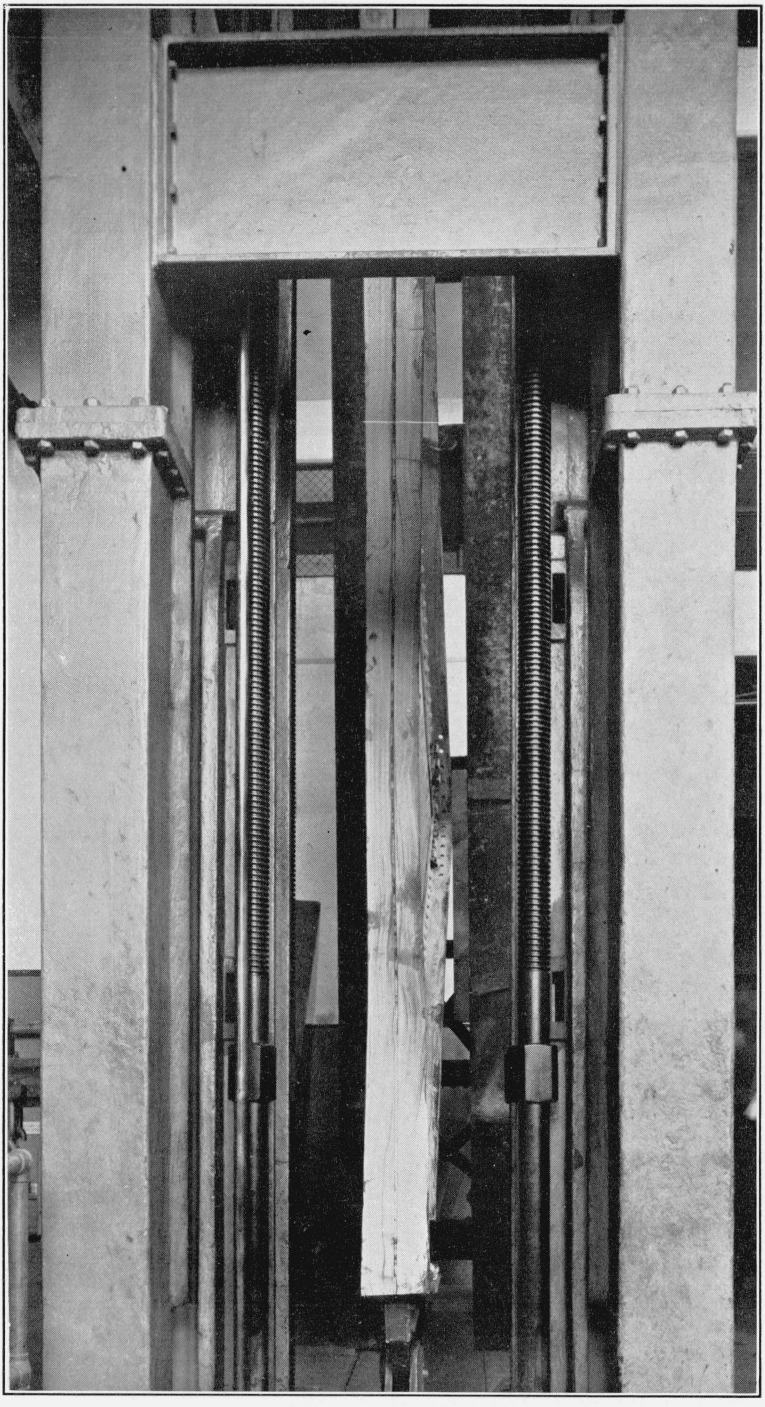

FIGURE 17.—*The rigid-frame specimen under the maximum load of 72,000 lb.*

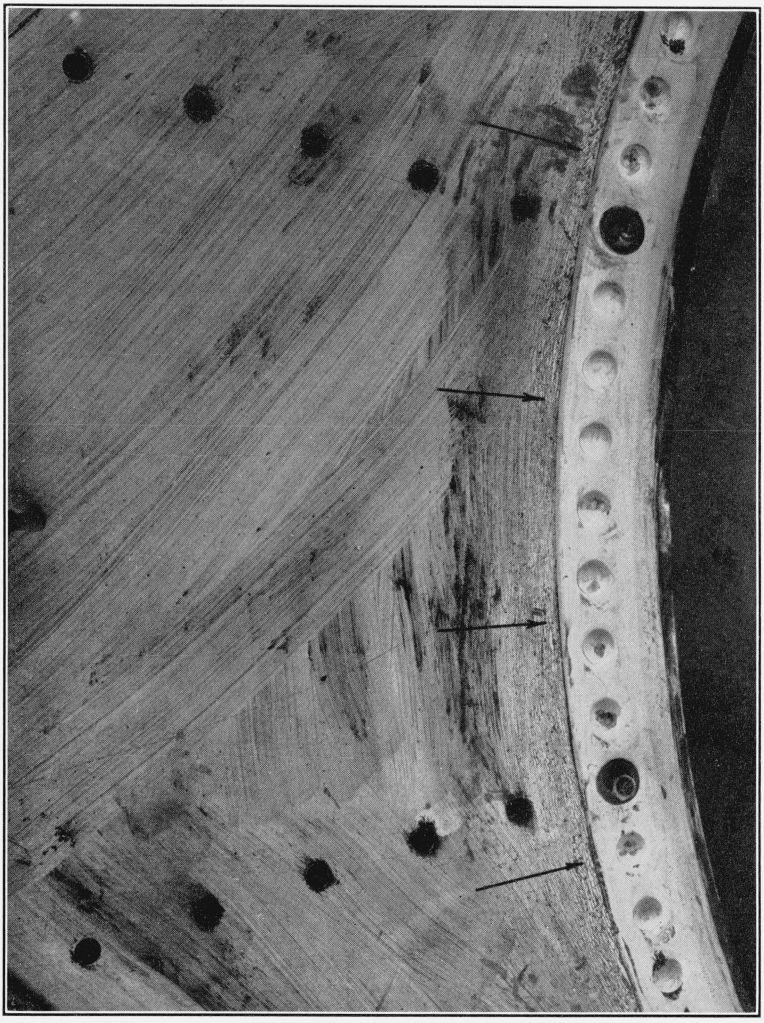

FIGURE 18.—*Inner portion of the rigid-frame specimen after failure.*
Lüders' lines are visible in a narrow band adjacent to the curved flange.

IX. REFERENCES

[1] Ambrose H. Stang, Martin Greenspan, and William R. Osgood, *Strength of a riveted steel rigid frame having straight flanges.* J. Research NBS **21**, 269 (1938) RP1130.
[2] *Standard specifications for steel for bridges.* Fig. 1, A. S. T. M. Standards, pt. I, 4 (1936).
[3] L. B. Tuckerman, *Discussion on proportional limit.* Proc. Am. Soc. Testing Materials **29**, II, 538 (1929).
[4] S. Timoshenko, Theory of Elasticity (McGraw-Hill Book Co., Inc., 1934).

WASHINGTON, August 5, 1938.